

Spontaneous rearrangement of the checkerboard charge order to stripe order in $\text{La}_{1.5}\text{Sr}_{0.5}\text{NiO}_4$

R. Kajimoto,¹ K. Ishizaka,² H. Yoshizawa,³ and Y. Tokura²

¹*Department of Physics, Ochanomizu University, Bunkyo-ku, Tokyo 112-8610, Japan*

²*Department of Applied Physics, University of Tokyo, Bunkyo-ku, Tokyo 113-8656, Japan*

³*Neutron Scattering Laboratory, ISSP, University of Tokyo, Tokai, Ibaraki 319-1106, Japan*

(Dated: February 1, 2008)

The charge ordering in $\text{La}_{1.5}\text{Sr}_{0.5}\text{NiO}_4$ has been studied with neutron diffraction technique. An interesting rearrangement of the charge ordering was observed as a function of temperature. With decreasing temperature, a checkerboard-type charge order is formed below $T_{\text{CO}}^{\text{C}} \sim 480$ K. It is, however, taken over by the stripe-type charge order with an incommensurability twice as large as that of the spin order below $T_{\text{CO}}^{\text{IC}} \sim 180$ K. Surprisingly, the stripe phase persists up to $x = 0.7$ for highly hole-doped samples of $\text{Nd}_{2-x}\text{Sr}_x\text{NiO}_4$ with $0.45 \leq x \leq 0.7$.

PACS numbers: 75.25.+z, 71.27.+a, 71.45.Lr, 74.80.Dm

One of the most fascinating examples of charge ordering may be a so-called stripe order discovered in the high- T_c superconducting cuprates.¹ Recent studies have revealed that the stripe order cannot be simply attributed to the Coulomb interactions, but is a consequence of an interplay among spin, charge, and lattice degrees of freedom. A stripe order is also known to exist in the isostructural nickelates, although its stripe order is relatively static compared with that of the cuprates. In hole-doped nickelates $\text{La}_{2-x}\text{Sr}_x\text{NiO}_{4+\delta}$, the static stripe order is observed for a wide hole concentration region $0.15 \lesssim n_h \leq 1/2$,^{2,3} where $n_h = x + 2\delta$. In the stripe ordered state, the doped holes form charge stripes characterized by a modulation vector $\mathbf{g}_{\text{CO}} = (2\epsilon, 0, 0)$ in the orthorhombic lattice units ($a_o = \sqrt{2}a_t$). The Ni spins order antiferromagnetically with antiphase domain boundaries on the charge stripes. The modulation vector of the spin order thus becomes $\mathbf{g}_{\text{SO}} = \mathbf{Q}_{\text{AF}} \pm (\epsilon, 0, 0)$, where $\mathbf{Q}_{\text{AF}} = (1, 0, 0)$ is the wave vector for a simple antiferromagnetic order. The incommensurability ϵ keeps a linear relation to n_h for $n_h \leq 1/2$, $\epsilon \sim n_h$.^{2,3} The stripe order is most stable at $\epsilon = 1/3$ where it shows the highest charge and spin ordering temperatures and the longest correlation length. Moreover, ϵ exhibits a systematic deviation from the linear relation around $n_h \sim 1/3$ by approaching $\epsilon = 1/3$, which manifests the quite unique nature of the stripe order in the Sr-doped nickelate system.^{4,5}

On the other hand, another well-known ground state of a hole doped system is a so-called checkerboard-type charge order. The doping concentration of 50% holes is ideal for the checkerboard charge order, and this charge order is widely seen in isostructural transition metal oxides with $n_h = 1/2$ such as manganites⁶ and cobalates.⁷ Note that the $\epsilon = 1/2$ -limit of the stripe order in nickelates coincides with the checkerboard charge order. Early electron diffraction and transport studies,^{8,9} indeed, indicated the existence of a checkerboard charge order at $n_h = 1/2$. From our recent studies on the highly Sr-doped nickelate system, however, we failed to detect any superlattice peaks from the incommensurate or checker-

board charge order in the $x = 1/2$ sample.³ Instead, we observed an *incommensurate spin* order with an incommensurability $\epsilon \sim 0.44$ (see Fig. 2(c)).³ Surprisingly, the stripe order persists even at $n_h = 1/2$, and this result gives rise to a question whether the ground state of the nickelates at $n_h = 1/2$ is the checkerboard charge order or stripe charge order.

In the present study, we solve such a mystery of the charge ordering in the 50% doped nickelate, and demonstrate that the charge ordering shows an interesting rearrangement from a checkerboard charge order to a stripe order in the $x = 1/2$ Sr-doped nickelate. We found that the checkerboard charge order is formed at $T \sim 480$ K, but a part of the system changes over to the stripe-type charge order with decreasing T . This complicated behavior is a consequence of a strong correlation of the couplings between charge and spin degrees of freedom.

Large single crystal samples were grown by the floating zone method. They were pre-characterized by resistivity measurements, and cut into the size of $6\text{ mm}\phi \times 25\text{ mm}$ for the present neutron diffraction study. The neutron diffraction experiments were performed using triple axis spectrometer GPTAS installed at the JRR-3M reactor in JAERI, Tokai, Japan with a fixed incident neutron momentum of $k_i = 3.81\text{ \AA}^{-1}$. We chose a combination of horizontal collimators of $40'-40'-40'-80'$ (from monochromator to detector), and set two PG filters before the in-pile and after the sample positions to eliminate higher order contaminations. The temperature of the sample was controlled by a high temperature-type closed-cycle He gas refrigerator within an accuracy of 0.2 K. Although the crystal has a tetragonal structure (space group $I4/mmm$), we employ a larger unit cell of the size $\sqrt{2}a_t \times \sqrt{2}a_t \times c_t$ relative to the simple $I4/mmm$ lattice.

We first show the temperature (T) dependence of the in-plane resistivity within the ab plane ($\mathbf{j} \perp c$) of our $\text{La}_{1.5}\text{Sr}_{0.5}\text{NiO}_4$ sample in Fig. 1. Though the resistivity is almost metallic at high temperature ($\rho(600\text{ K}) \sim 2.5 \times 10^{-3}\text{ \Omega cm}$), it still increases monotonically as T is lowered. A careful examination of the T derivative of

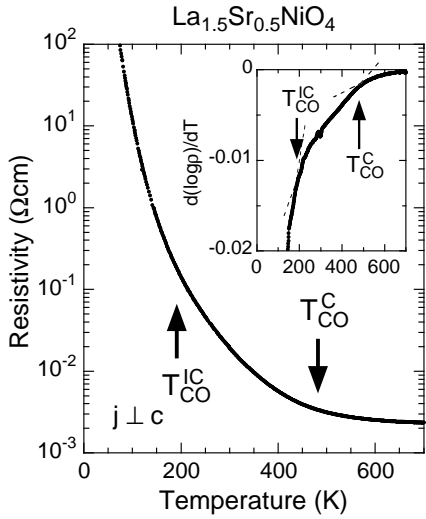


FIG. 1: Temperature dependence of the resistivity within NiO_2 plane (main panel) and its temperature derivative (inset).

the resistivity, $d \log \rho / dT$ (inset) suggests that the T dependence of the resistivity changes its slope twice: the first clearer change locates at $T_{\text{CO}}^{\text{C}} \sim 480 \text{ K}$, and the second crossover-like change occurs at $T_{\text{CO}}^{\text{IC}} \sim 180 \text{ K}$. We note that the anomaly at $T_{\text{CO}}^{\text{C}} \sim 480 \text{ K}$ is substantially higher than the anomaly reported in early studies of the resistivity and electron diffraction patterns,^{8,9} and that the one at $T_{\text{CO}}^{\text{IC}} \sim 180 \text{ K}$ is recognized for the first time in the present study. It is possible that these anomalies in the resistivity corresponds to a two-step process of the charge localization, and they may indicate that two different types of charge ordering are formed below the temperatures of two respective anomalies.

In order to find signals due to possible charge orderings inferred by the anomalies of the resistivity, we surveyed reciprocal lattice positions around $(h, k, 0)$ with $h + k = \text{odd}$, where superlattice peaks due to the checkerboard charge order are expected. Figures 2(a) and (b) show scan profiles along the $[100]$ direction around $(5, 0, 0)$ and $(4, 3, 0)$ at several T 's. In Fig. 2 (c) is also shown a profile of a magnetic peak at $(1, \epsilon, 0)$ measured along the $[010]$ direction at 10 K. In Figs. 2(a) and (b), quite sharp peaks appear at commensurate positions at $(5, 0, 0)$ and $(4, 3, 0)$ below T_{CO}^{C} . These profiles clearly demonstrate that the checkerboard charge ordering is formed in our $x = 1/2$ sample below T_{CO}^{C} , consistent with the early electron diffraction experiment.⁸

More importantly, a pair of satellite peaks emerges below $T_{\text{CO}}^{\text{IC}}$ on both sides of the commensurate checkerboard charge order superlattice peaks with further lowering T , as indicated by arrows in Figs. 2(a) and 2(b) ($h \sim 5 \pm 0.13$ and $h \sim 4 \pm 0.13$, respectively). With use of the incommensurability of the magnetic reflections $\epsilon \sim 0.44$, the satellite peaks are indexed as $(h \pm 2\epsilon, k, 0)$ with $h + k = \text{even}$. Thereby, we identify them as the

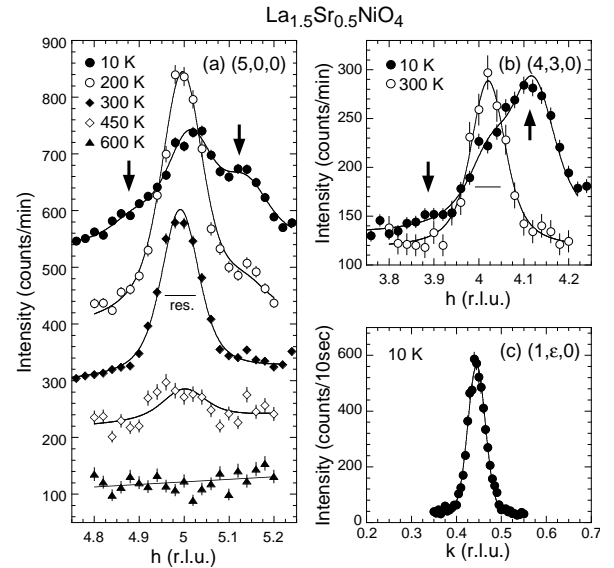


FIG. 2: (a), (b) Temperature dependences of the profiles of charge order peaks at and around $(5, 0, 0)$ (panel (a)) and $(4, 3, 0)$ (panel (b)). (c) Profile of a spin order peak $(1, 0.44, 0)$ at 10 K. In the panel (a), the y axis is sifted by 100 counts for each data. Horizontal bars and solid lines in the panel (a) and (b) indicate the instrumental resolutions (FWHM) and Lorentzian profiles convoluted with the instrumental resolution, respectively. A solid line in the panel (c) is a fit to a Gaussian.

charge and spin superlattice peaks from the stripe-type charge order with $\epsilon \sim 0.44$. These observations lead us to conclude that the two types of charge order coexist at low temperatures in the Sr-doped nickelate with $n_h = 1/2$.

To determine correlation lengths within the NiO_2 planes, the profiles of the charge order peaks in Fig. 2 are fitted to a Lorentzian form with the instrumental resolution. The correlation length for the checkerboard charge order becomes $\xi_{\text{CO}}^{\text{C},h} \approx 40 \text{ \AA}$ at 300 K, but is reduced to $\approx 20 \text{ \AA}$ at 10 K following the development of the stripe charge order below $T_{\text{CO}}^{\text{IC}}$. At 10 K, the correlation length of the stripe charge order $\xi_{\text{CO}}^{\text{IC},h}$ is $\approx 20 \text{ \AA}$. Both $\xi_{\text{CO}}^{\text{C},h}$ and $\xi_{\text{CO}}^{\text{IC},h}$ are nearly equal, but much shorter than the correlation length of the spin order $\xi_{\text{SO}}^h \approx 120 \text{ \AA}$ (10 K).³ It should be noted that $\xi_{\text{CO}}^{\text{C},h}$ is also very close to the literature value for the checkerboard charge order in $\text{La}_{1.5}\text{Sr}_{0.5}\text{CoO}_4$, $26(2) \text{ \AA}$.⁷ We also measured the profiles of the charge order peaks along the $[001]$ direction to examine the stacking of the charge order (not shown). We found the scattering intensity of either type of charge ordering has a very weak l dependence. The profile of the checkerboard order exhibits peaks at $l = \text{even}$ positions, while that of the stripe order shows a weak bump at $l = \text{odd}$. From the observed profiles, we estimate the out-of-plane correlation length of the checkerboard charge order $\xi_{\text{CO}}^{\text{C},l}$ is $\sim 1 \text{ \AA}$ at 300 K and $\sim 2 \text{ \AA}$ at 10 K, while that of the stripe order $\xi_{\text{CO}}^{\text{IC},l}$ is $\sim 3 \text{ \AA}$ at 10 K. For the checker-

board charge order, the stacking along the [100] direction and that along the [010] direction are equivalent, because the arrangement of the charges is isotropic within NiO_2 planes. Quite short correlation length of the spin and charge stripe order between NiO_2 planes is likely caused by a frustration of the stacking of the charge stripes.

In order to examine an ordering process of the two charge orders, the T dependencies of the intensity of the commensurate peak at $(5, 0, 0)$ and the satellite peak at $(4.13, 3, 0) = (5 - 2\epsilon, 3, 0)$ are depicted in Fig. 3. With decreasing T , the intensity at $(5, 0, 0)$ starts to grow around $T_{\text{CO}}^{\text{C}} \sim 480$ K.¹⁰ This temperature is in good agreement with the anomaly in the resistivity (Fig. 1), but is much higher than the charge ordering temperature reported in Ref. 8. Further decreasing T , the intensity reaches a maximum around $T_{\text{CO}}^{\text{IC}} \sim 180$ K, and then turns to decrease below $T_{\text{CO}}^{\text{IC}}$. The maximum of the commensurate component is well correlated with the onset of the satellite (incommensurate) components. The intensity of the satellite peak at $(4.13, 3, 0)$ gradually develops below $T_{\text{CO}}^{\text{IC}}$. Clearly, this temperature coincides with the second anomaly in the resistivity shown in Fig. 1. In addition, the stripe spin order sets in at much lower temperature $T_N \sim 80$ K (see the inset of Fig. 3(b)). These T -dependent behaviors of the stripe charge and spin order manifest the marvelous stability of the stripe order at the commensurate hole concentration $n_h \sim 1/2$ in the Sr-doped nickelate.

The robustness of the stripe order observed in the $x = 1/2$ sample motivated us to investigate the higher doping region for $x > 1/2$. From our preliminary neutron diffraction measurements on the $\text{Nd}_{2-x}\text{Sr}_x\text{NiO}_4$ system, we found that the well-defined stripe-type order persisted even in the samples with the Sr concentration as high as $x = 0.7$. We also observed a weak signal of the checkerboard charge ordering in the $x = 0.6$ sample. The observation of the stripe ordering for $x \gtrsim 1/2$ is itself very unusual, and the nature of this stripe ordering deserves further experimental and theoretical studies.

In Fig. 4, we summarize the ordering temperatures $T_{\text{CO}}^{\text{IC}}$, T_{CO}^{C} and T_N , and the incommensurability ϵ of the stripe ordering in $\text{La}_{2-x}\text{Sr}_x\text{NiO}_{4+\delta}$ as well as $\text{Nd}_{2-x}\text{Sr}_x\text{NiO}_4$ as a function of the hole concentration n_h . All of these values for the Nd samples are in excellent accord with those for the La samples. As reported previously,³ ϵ shows a systematic deviation from the linear relation of $\epsilon = n_h$ around $n_h = 1/3$. Interestingly, we found that ϵ saturates for $x \geq 1/2$ with the value $\epsilon \sim 0.44$ as shown in the lower panel of Fig. 4. This result manifests that the stripe state is robust against the hole doping even for $n_h \gtrsim 1/2$, and may indicate that the electronic state for $x > 1/2$ is similar to that of $x = 1/2$. The details of the charge and spin ordering at $x > 1/2$ will be reported elsewhere.¹¹

Next, we discuss the ordering process of the charge and spin ordering in $x = 1/2$. The incommensurate charge ordering in $x = 1/2$ can be understood in terms of a discommensuration picture of the stripe ordering intro-

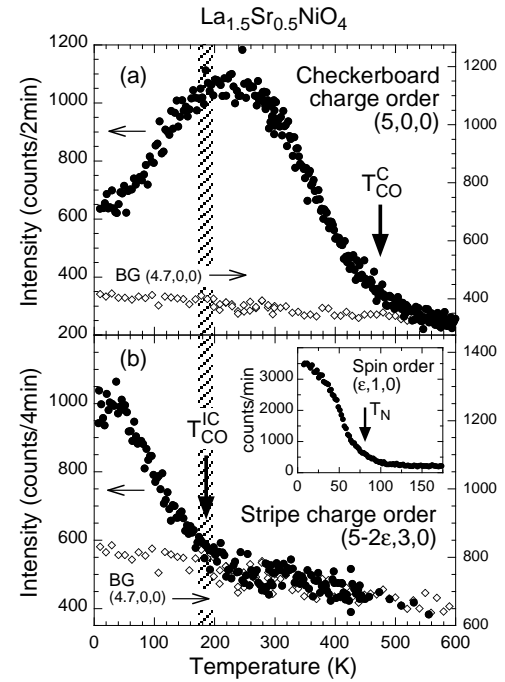


FIG. 3: Temperature dependencies of the peak intensities of the commensurate charge order peak $(5, 0, 0)$ (a) and stripe charge order peak $(4.13, 3, 0)$ (b). The background intensities measured at $(4.7, 0, 0)$ are also depicted. The inset in (b) is the temperature dependence of the peak intensity of the stripe spin order peak at $(0.44, 1, 0)$.

duced in our previous study.³ An example of the stripe order near $n_h = 1/2$ is illustrated in Fig. 5, based on the discommensuration picture. The checkerboard charge order consists of a matrix of the $\uparrow \times \bigcirc \times \downarrow$ pattern where arrows represent the spin direction on Ni^{2+} sites, while \times and \bigcirc symbols denote the oxygen sites and a hole on the Ni sites, respectively. The width of the unit cell of this ordering pattern becomes a as illustrated in Fig. 5(a). In the next step, a discommensuration will be introduced to such a pattern. For this purpose, an object of size $3a/2$ containing one hole (shaded areas in Figs. 5(b) and 5(c)) will be embedded for every three checkerboard units. The hole at each discommensuration region may occupy either a Ni site as $\bigcirc \times \uparrow \times \downarrow \times \bigcirc$ (Fig. 5(b)) or an oxygen site as $\uparrow \times \downarrow \otimes \downarrow \times \uparrow$ (Fig. 5(c)). It should be noted that one cannot determine whether a hole occupy a Ni site or an oxygen site in the discommensuration region only from the present study, although O-centered discommensuration may be preferred by the Coulomb repulsion between the holes. In any event, the introduction of the discommensuration leads to an incommensurate (stripe) charge ordering with the incommensurability $\epsilon = (3 + 1)/(2 \times 3 + 3 \times 1) = 4/9 = 0.44$, being consistent with our observations.

An important result of the discommensuration is the energy gain by the spin exchange interactions. For the checkerboard charge ordered state, the exchange inter-

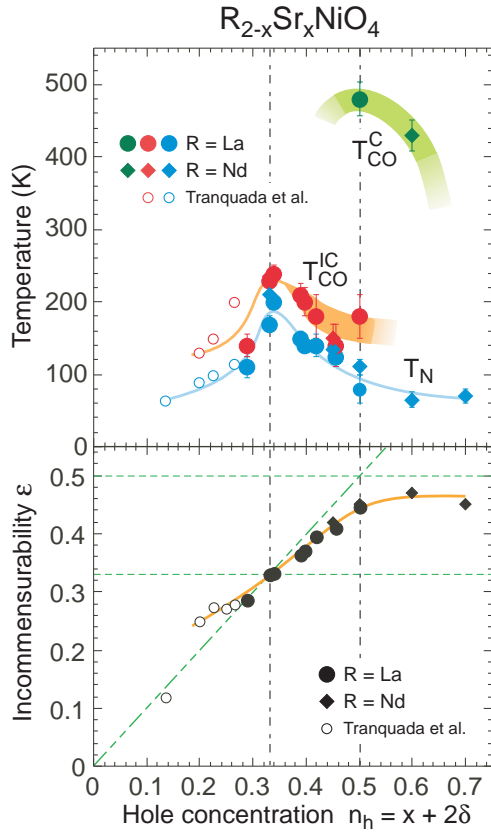


FIG. 4: (color) Phase diagram of $R_{2-x}Sr_xNiO_4$: (a) Hole concentration dependence of the transition temperatures, T_{CO}^{IC} , T_{CO}^C and T_N . For details, see text. (b) Hole concentration dependence of the incommensurability ϵ . Circles denote the data for $La_{2-x}Sr_xNiO_4$, while diamonds for $Nd_{2-x}Sr_xNiO_4$. Open symbols are taken from Ref. 2.

action between the nearest neighbor sites is unique, and there is only the one between Ni^{2+} and Ni^{3+} ions. By contrast, when the charge order becomes incommensurate, other kinds of exchange interactions between Ni ions can be introduced in the discommensuration regions: the Ni-centered discommensuration yields Ni^{2+} – Ni^{2+} bonds (Fig. 5(b)) while Ni^{2+} –hole– Ni^{2+} bonds are brought about by the O-centered discommensuration (Fig. 5(c)). Because the exchange interactions for these bonds are expected to be much stronger than that between Ni^{2+} and Ni^{3+} ,¹² the energy gain due to the spin exchange interactions is larger in the stripe state, and favors the stripe order.

From these considerations, a possible scenario of the ordering process of the charge ordering in the 50%-doped nickelate is as follows: At high T where the spin exchange interactions are disturbed by thermal fluctuations, small polarons are created through the electron-phonon coupling and they form the checkerboard order due to the Coulomb interactions between polarons.¹² With decreasing T , however, the spin correlation develops, and eventually a large energy gain of the Ni^{2+} – Ni^{2+} bonds stabilizes

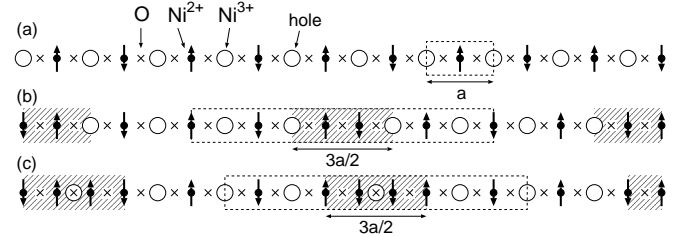


FIG. 5: Model patterns of the charge ordering in the NiO_2 plane along the [100] direction for the commensurate charge ordered state (a) and the incommensurate charge ordered state for $\epsilon = 4/9$ (b), (c). Small filled circles with arrows, open circles and crosses denote Ni^{2+} sites, holes, and oxygen sites, respectively. Arrows indicate the spin directions of the Ni^{2+} sites. Broken lines outline the unit cell of the charge ordering. The holes in the discommensuration region (shaded areas) occupy the metal sites in (b) while the oxygen sites in (c).

the stripe order by introducing holes into the checkerboard pattern. Although the checkerboard charge order is favored by *charges*, it is further disfavored by the *spin* exchange interactions. The latter favors the incommensurate ordering and results in the coexistence of the commensurate and stripe ordered regions at low temperatures in the nickelate system for $x \gtrsim 1/2$. The present observation suggests the importance of the role of the spin exchange interactions in the charge ordering in the Sr-doped nickelate system.

It would be interesting to compare the present stripe formation at $x = 1/2$ with the appearance of the stripe phase in a cuprate with a very low hole concentration. Very recently, Matsuda *et al.* revealed that a lightly-doped $La_{2-x}Sr_xCuO_4$ with $x < 0.02$ shows a phase separation between a non-doped Néel ordered region and a diagonal stripe-phase region with $\epsilon \sim 0.02$.¹⁴ In the lightly-doped cuprates, the stripe with a modulation of $\epsilon \sim 0.02$ emerges from the matrix of the non-doped Néel ordered state, while in the nickelate with $x = 1/2$, the stripes emerge from the matrix of the checkerboard charge order, and result in an antiphase domain modulation with a propagation vector of $1/2 - \epsilon \sim 0.05$. In this sense, the present results for the $n_h = 1/2$ nickelate can be regarded as a counterpart of the behavior of the cuprate with $n_h \lesssim 0.02$. We would like to suggest that, in general, a stripe phase is magnetically favored more than the state with a homogeneous hole distribution even in the limiting case of 0% or 50% doping.

In conclusion, we observed in $La_{1.5}Sr_{0.5}NiO_4$ a rearrangement of the checkerboard-type charge ordering to the stripe-type one. With decreasing T , a checkerboard charge order is formed below $T_{CO}^C \sim 480$ K. This charge order is, however, taken over by the stripe-type charge order with an incommensurability twice as large as that of the spin order below $T_{CO}^{IC} \sim 180$ K. The stripe ordered phase survives up to $x = 0.7$ in $Nd_{2-x}Sr_xNiO_4$. These results evidence the unusual robustness of the stripe order,

and suggest the importance of the interactions between spins and charges in the Sr-doped nickelate system.

Acknowledgments

The authors thank K. Chatani and K. Hirota for a loan of the high temperature-type closed cycle He gas

refrigerator. This work was supported by a Grant-In-Aid for Scientific Research from the Ministry of Education, Culture, Sports, Science, and Technology, Japan and by the New Energy and Industrial Technology Development Organization (NEDO) of Japan.

¹ J. M. Tranquada, B. J. Sternlieb, J. D. Axe, Y. Nakamura, and S. Uchida, *Nature (London)* **375**, 561 (1995).

² J. M. Tranquada, D. J. Buttrey, and V. Sachan, *Phys. Rev. B* **54**, 12318 (1996).

³ H. Yoshizawa, T. Kakeshita, R. Kajimoto, T. Tanabe, T. Katsufuji, and Y. Tokura, *Phys. Rev. B* **61**, R854 (2000).

⁴ T. Katsufuji, T. Tanabe, T. Ishikawa, S. Yamanouchi, Y. Tokura, T. Kakeshita, R. Kajimoto, and H. Yoshizawa, *Phys. Rev. B* **60**, R5097 (1999).

⁵ R. Kajimoto, T. Kakeshita, H. Yoshizawa, T. Tanabe, T. Katsufuji, and Y. Tokura, *Phys. Rev. B* **64**, 144432 (2001).

⁶ B. J. Sternlieb, J. P. Hill, U. C. Wildgruber, G. M. Luke, B. Nachumi, Y. Moritomo, and Y. Tokura, *Phys. Rev. Lett.* **76**, 2169 (1996).

⁷ I. A. Zaliznyak, J. P. Hill, J. M. Tranquada, R. Erwin, and Y. Moritomo, *Phys. Rev. Lett.* **85**, 4353 (2000).

⁸ C. H. Chen, S-W. Cheong, and A. S. Cooper, *Phys. Rev. Lett.* **71**, 2461 (1993).

⁹ S-W. Cheong, H. Y. Hwang, C. H. Chen, B. Batlogg, L. W. Rupp, Jr., and S. A. Carter, *Phys. Rev. B* **49**, 7088 (1994).

¹⁰ Due to the short range nature of charge orderings, the scattering intensity of the superlattice peaks do not show clear anomalies through the transition temperatures. We define T_{CO} 's as temperatures below which the intensity increases with logarithmic T dependence (see Ref. 5).

¹¹ K. Ishizaka *et al.*, unpublished.

¹² J. Zaanen and P. B. Littlewood, *Phys. Rev. B* **50**, 7222 (1994).

¹³ K. Yamada, C. H. Lee, K. Kurahashi, J. Wada, S. Wakimoto, S. Ueki, H. Kimura, Y. Endoh, S. Hosoya, G. Shirane, R. J. Birgeneau, M. Greven, M. A. Kastner, and Y. J. Kim, *Phys. Rev. B* **57**, 6165 (1998).

¹⁴ M. Matsuda, M. Fujita, K. Yamada, R. J. Birgeneau, Y. Endoh, and G. Shirane, *Phys. Rev. B* **65**, 134515 (2002).